19th Brazilian Congress of Thermal Sciences and Engineering
November 06th-10th, 2022, Bento Gonçalves - RS - Brazil

ENC-2022-0213
INTERFACE TEMPERATURE MEASUREMENTS AND CRYSTAL VISUALIZATION DURING WAX DEPOSIT FORMATION ON COLD SURFACES

Ricardo Cavalcanti Linhares
Luis Fernando Alzuguir Azevedo
Pontifícia Universidade Católica do Rio de Janeiro. Rua Marquês de São Vicente, 225, Gavea, Rio de Janeiro, Brazil.
ricklinhares@gmail.com; lfaa@puc-rio.br

Felipe Pereira Fleming
CENPES, Petrobras Research and Development Center, Rio de Janeiro 21914-915, Brazil
ffleming@petrobras.com.br

Abstract. *Wax deposition in pipelines is a critical problem for the oil and gas industry. The correct prediction of the wax buildup is important for the planning stages of new projects and optimization of pig's passage. The current wax deposition models, widely used in the oil industry, do not incorporate the complete deposition mechanisms, relying on adjusting parameters that are specific of particular fields from where the data were obtained. For that reason, their predictions are not sufficiently accurate and cannot be extrapolated to other fields. In the present work a study was conducted to contribute to the understanding of the basic deposition mechanism. To this end, a test section with a simple geometry, well controlled conditions and a model oil with known proprieties were employed. The measurements obtained were used to validate simulation models and provide valuable information on the wax deposition mechanisms. A miniature probe was developed to measure the evolution of the deposit-liquid interface temperature and deposit thickness for three different Reynolds numbers in the laminar regime. Differently from what is found in the literature, the deposit-liquid interface temperature was found to increase from the wax appearance temperature (WAT) to a temperature value between the WAT and the wax disappearance temperature (WDT). The finding that the deposit-liquid interface temperature never below the WAT, indicate that, for the range of operating conditions of the present experiments, the main mechanism responsible for the deposit growth is heat-transfer-induced phase change, while molecular diffusion becomes more important in later stages for the deposit aging process. Using a high resolution camera, the transparent plexyglass test section allowed for the acquisition of original images of the deposit formation and growth, as well as the visualization of wax crystals flowing in suspension above the deposit. The images also show the competition between the yield stress of the newly formed deposit and the shear stress imposed by the flowing oil.*

Keywords: *Wax deposition; petroleum pipelines; flow assurance; flowing crystals; interface temperature.*

1. INTRODUCTION

One of the most significant problems for the production and transportation of petroleum is the formation of paraffin deposits on the internal walls of pipelines. The formation of these wax deposits results on the reduction of the cross section of the pipelines increasing the pressure drop of the transportation lines and, consequently, reducing the production rate and increasing pumping power. Depending on wax content of the oil and the environmental conditions surrounding the pipelines, the wax deposition problem may become critical, leading to the total blockage of the line. With production reaching ever greater depths and longer tiebacks, as seen in the Brazilian pre-salt fields, conditions for wax deposition problems are favored. The ability to predict wax deposition is of fundamental importance in the design stages of a pipeline. Also, the design of wax removal operations relies on good estimates of wax deposition rates. The most common method to remove wax deposits from pipelines is through pipeline pigging (Gao et al., 2021). The advance knowledge of the wax deposit thickness and mechanical resistance is also relevant information. It is known that over time, the heavier components of the solution diffuse into the deposit while the lighter fractions diffuse out, causing an increase in its hardness, what is known as deposit aging. Aged deposits offer increased resistance to removal by pigging operations (Hoteit et al., 2008; Merino-Garcia et al., 2007; Singh et al., 2001; Veiga et al., 2020).

There are currently a few commercial software that attempt to predict wax deposition, however there is still not a well –accepted model that can accurately predict the wax deposit evolution in different field conditions. The major challenge is to identify the dominant deposition mechanisms to be implemented in these models. Initially in the literature there were assumptions that gravity settling, Brownian diffusion, and thermophoresis could be relevant, but these mechanisms were readily disregarded as significant contributors to this problem. The main mechanism that has been considered for decades as the main responsible for wax deposition is molecular diffusion (Burger et al., 1981; Hamouda & Ravnøy, 1992; Hoffmann & Amundsen, 2010; Singh et al., 2000).

A few authors in the last decades have questioned the acceptance of molecular diffusion as the main deposition mechanisms. The practice of adjusting the predictions of the models to field and laboratory data have made the molecular diffusion model widely employed (Azevedo & Teixeira, 2003). These tuning parameters appeared in different forms, such as kinetic coefficients (Huang et al., 2011), adjusting constants (Alhosani & Daraboina, 2020) or by simply adjusting the molecular diffusion coefficient to fit the wax deposit found experimentally (Singh et al., 2000). The fact that molecular diffusion alone is not sufficient to predict the evolution of deposits is an indication that other mechanisms are missing from the modeling (Soedarmo et al., 2017). In recent years the acceptance that other mechanisms might be relevant in wax deposition have appeared more frequently in the literature (Mahir et al., 2019; van der Geest et al., 2021; Van Der Geest et al., 2018; Yang et al., 2020).

Wax deposition has also been treated as controlled solely by heat transfer (Bhat & Mehrotra, 2004; H. O. Bidmus & Mehrotra, 2004; Parthasarathi & Mehrotra, 2005)(Bhat & Mehrotra, 2004; Parthasarathi & Mehrotra, 2005). In this line of work, the numerical simulations consider that wax deposition is a phase change problem, only taking into account the heat transfer as responsible for the formation of wax deposits. Models based on this assumption were developed and compared to experimental data mostly obtained from flow loop test sections (Ehsani et al., 2019a; Ehsani & Mehrotra, 2020; Haj-Shafiei & Mehrotra, 2019; Mehrotra & Bhat, 2007; Tiwary & Mehrotra, 2009) or cold finger devices (Ehsani et al., 2019b; Ehsani & Mehrotra, 2019; Haj-Shafiei & Mehrotra, 2019). Several experiments performed indicated that the wax deposit interface evolves at the e wax appearance temperature (WAT), supporting the assumption that heat transfer is the only responsible for wax deposits formation (Mehrotra et al., 2020).

An important region that could provide valuable insight into this matter is the deposit-liquid interface. In the molecular diffusion modeling approach, for a concentration gradient to occur, the temperature of the deposit-liquid interface must always be below the WAT, while in the case of modeling the deposition only by heat transfer the deposit-liquid interface must always follow the WAT.

Bidmus & Mehrotra (2008a, 2008b) attempted to make measurements on the deposit-liquid interface using 3.2–mm-diameter thermocouples. However, the temperature data was not registered when these rather large thermocouples tips were visualized inside the deposit-liquid interface. Instead, the temperature data was later analyzed *a posteriori* and the deposit-liquid interface was assumed to be the region where the highest temperature gradient occurred. Moreover, the experiments were performed in a closed vessel and the test solution could be depleted as the deposition time and thickness increased.

The rheological characteristics of the deposits have also been recently considered as relevant to determine the deposit formation (Mahir et al., 2019; Palermo & Tournis, 2015; Zheng et al., 2017). In this modelling approach, the deposit is formed when the yield stress of the deposit is higher than the shear stress imposed by the flowing oil at the interface. The yield stress can be obtained by the rheological tests and can be associated with the solid fraction prevailing in the deposit.

As could be seen in this brief literature review, there is not yet a consensus on the mechanisms responsible for wax deposition. The accurate measurements of the temperature of the deposit-liquid interface can provide valuable insights on the mechanisms responsible for wax deposition. In this work we successfully measured the region of the deposit-liquid interface without interrupting the deposition process and without disturbing the deposition site. The measurements were carried out with a retractable miniature probe, in a well-controlled test section employing a test fluid with known properties.

The use of a high resolution digital camera, made it possible to visualize the precise moment that the temperature probe reached the deposit-liquid interface region. Original images of the wax deposit formation were obtained, showing that the rheological properties do play a role in the deposition process. In these videos it is possible to see suspended wax crystals above the deposit and also the competition between the yield stress of the newly formed deposit and the shear stress of the flow.

2. METHODOLOGY

The experiments were carried out in a flow loop test section that was built in the Fluids Engineering Laboratory of Pontifical Catholic University (LEF/PUC-Rio). A schematic view of the experimental set-up can be seen in Figure 1. The arrangement consisted of an annular assembly, which will be later described in this section, fed by a cylindrical stainless steel tank filled with 23 L of the model oil. A magnetic heating plate was used beneath the storage in order to melt the test solution and to keep it homogenized during the experiments. The solution was pumped inside the annular assembly by a volumetric pump, Netzsch NEMO021, in order to provide a constant inlet flow rate condition. Heating tapes surrounding the rubber hoses were also activated in order to avoid any wax crystal formation. The tank where the annular

test section was installed was filled with water and a Haake DC30 thermostatic unit kept it at a controlled temperature of 38.6°C. Two thermostatic baths were used to alternate between pumping hot and cold water inside the internal pipe and a set of four ball valves were used to perform this transition. The temperatures of the two thermostatic baths were set, one at a hot temperature level of WAT+3°C, and the other at a cold temperature level of WAT-23.6°C. A temperature probe was located at 80% of the total length of the annular assembly. The arrows displayed in the Figure 1 indicate the flow direction of the fluids.

The annular assembly was formed by a pipe in pipe structure where the inner pipe was made of copper and the outer pipe was made of acrylic, forming a 7.5 mm annular gap. In the beginning of the experiments hot water would flow inside the copper pipe and hot wax solution would flow in the annular region between the copper and the acrylic. The experiment was initiated when cold water was pumped inside the inner pipe, rapidly decreasing the copper wall temperature and inducing the formation of wax deposit around it. The transparent acrylic pipe permitted the visualization of the entire deposition process, what not only allowed for more precise measurements of the interface temperature, but also yielded the acquisition of original images of the deposition process. In the location where the measuring temperature device were positioned, an acrylic block was machined in order to minimize optical distortions caused by curved acrylic pipe, thereby providing excellent images of the interior of the test section. The camera chosen for the experiments herein presented was the MotionPro X3 high speed camera. The 100-µm probe was initially retracted to avoid any disturbances on the flow, and at the desired deposition time, it was lowered until reaching the deposit liquid interface, while the temperature data was being registered. The exact moment that the tip of the probe entered the deposit-liquid interface region could be clearly visualized by the optical setup employed.

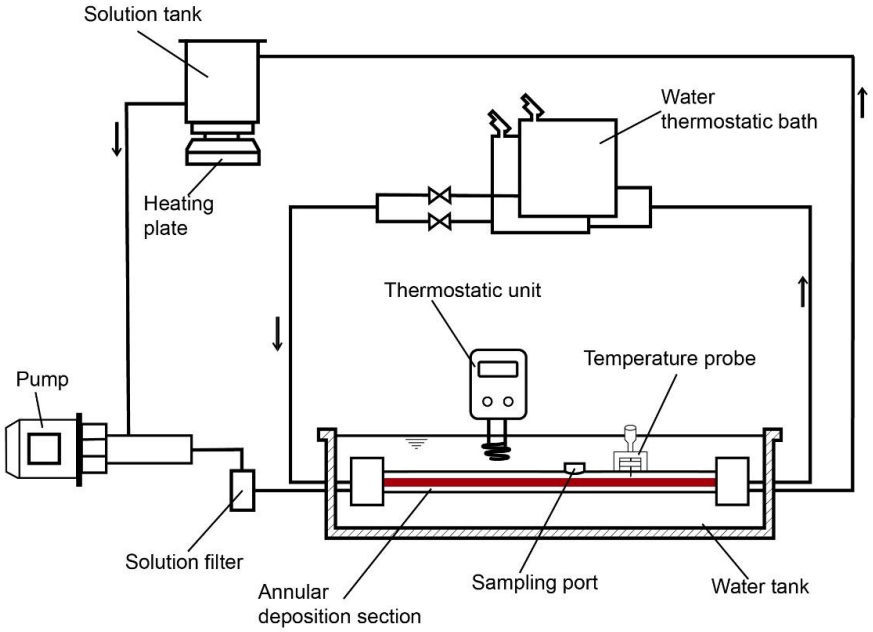

Figure 1 Schematic view of the test section employed in the wax deposition (Veiga et al., 2020).

The inner wall of the copper pipe was instrumented with 11 type-E thermocouples uniformly distributed along its length, with the thermocouple junctions installed in the copper wall so as not disturb the flow in the annular region. Thanks to this construction, it was possible to obtain precise data of the cooling rate being employed. The rapid ball valve maneuver that alternated between the two thermostatic baths resulted in a high cooling rate that consisted of two segments, as can be seen in Figure 2. In the first 40 seconds an abrupt temperature drop occurred, corresponding to a cooling rate of 32°C/min, followed by a lower cooling rate of 0.25 °C/min, after which the wall temperature reached its steady state value of 12°C.

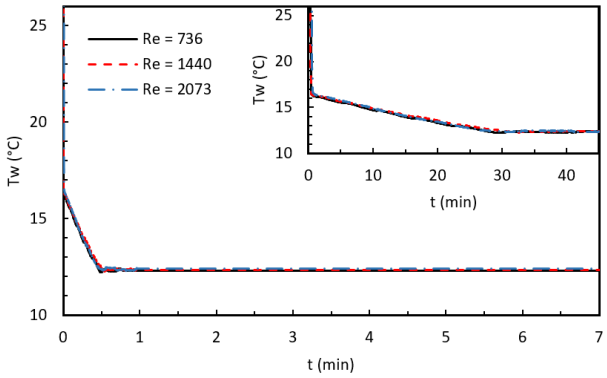

Figure 2: Temporal variation of the spatially-averaged copper pipe wall temperature, for Reynolds numbers 736, 1440 and 2073 (Veiga et al., 2020).

2.1 Test fluid

A model oil was used in the present work. The wax components in the test fluid solution were obtained by the distillation of a crude oil, so that there was a clear distinction between the paraffinic components (C22-C39) and the solvent (C12). The paraffinic components represent 20% of the total solution. The melting point of the mixture is 55.2°C and its density 747.8 kg/m3 at 40°C. The viscosity of the solution at 38°C was 1.462 mPa·s. The average molar mass of paraffin was 403.4 kg/mol, which corresponds to a carbon number of 28. The C_{12} was supplied by Shanghai IS Chemical Technology and its composition had 99% of purity. A chromatogram of the test fluid can be seen in Figure 3. The solvent (C12) percentage is presented at the left vertical axis while each of the paraffinic components (C22-C39) percentage is presented at the right vertical axis.

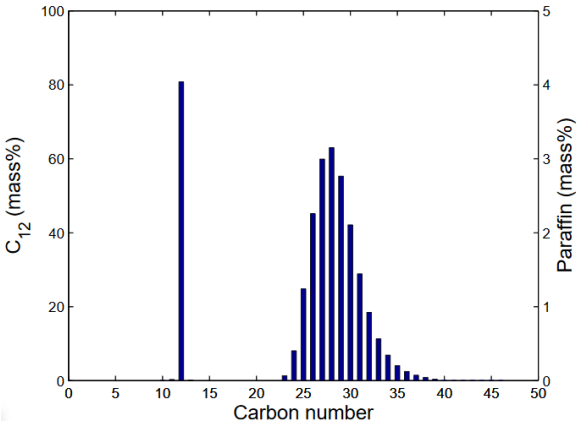

Figure 3 Chromatogram of the model oil employed in our test section (Veiga et al., 2020).

3. RESULTS AND DISCUSSION

In this section, the experimental results of the deposit liquid interface temperature and the visualization of the wax deposition process are presented.

3.1 Deposit-liquid interface temperature

The experiments were performed for three different Reynolds number values, namely 736, 1440 and 2073. As in these experiments a high cooling rate was employed, the deposit was rapidly formed. Temperature measurements were initially performed at 30-minute intervals for seven hours, with the exception of the first measurement, which was measured at 5 minutes after the beginning of the deposition. The uncertainty of the deposit-liquid interface temperature measurements was estimated to be ±0.3˚C.

The time evolution of the deposit-liquid interface temperature is shown in Figure 4 Figure 6. The black dashed horizontal lines at the bottom and top of the figures indicate the values of the measured WAT and WDT of the model oil being studied. The error bars indicate the estimated uncertainties of the experiments. The dotted red line indicates the average of the measurements acquired after 30 minutes. It can be seen that this average value is within the error bars of all the measurements except for the initial five minutes, indicating that the deposit-liquid interface temperature remains

constant after an initial stage of rapid growth. Another relevant aspect to be observed is that the interface temperature does not match either the WAT or the WDT.

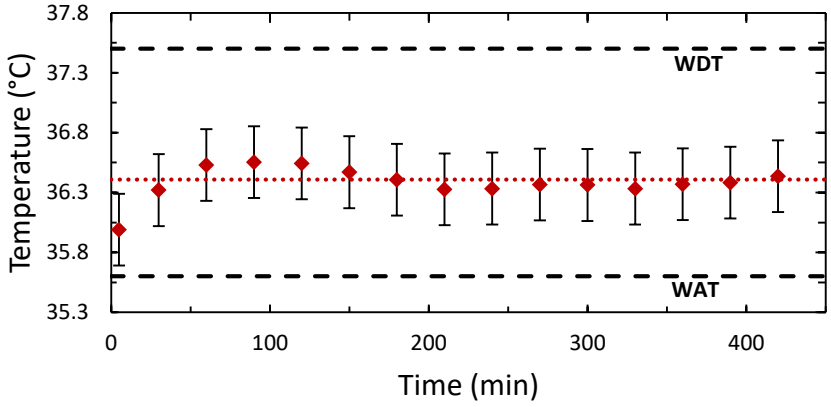

Figure 4: Time evolution of the deposit-liquid interface temperature for Reynolds number of 736.

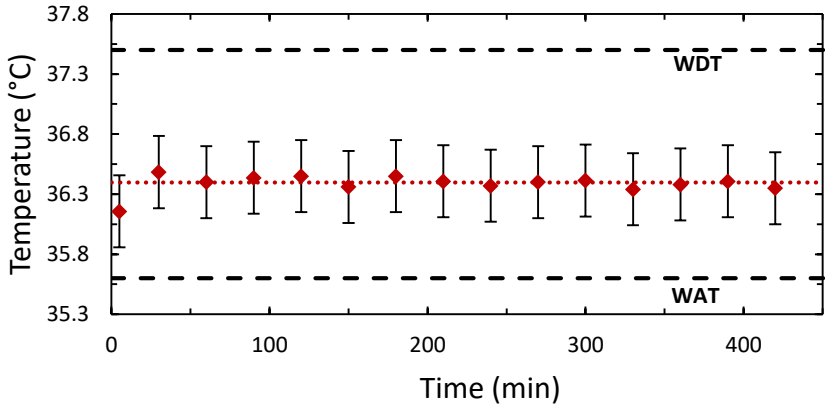

Figure: 5 Time evolution of the deposit-liquid interface temperature for Reynolds number of 1440.

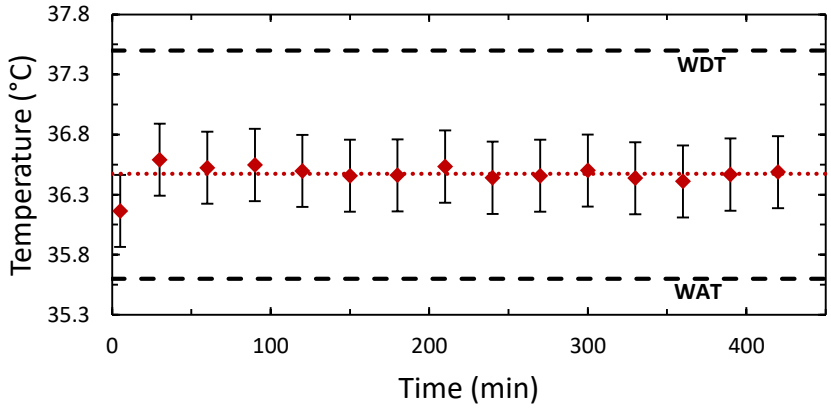

Figure 6: Time evolution of the deposit-liquid interface temperature for Reynolds number of 2073.

Figure 7 combines the data for the three values of the Reynolds numbers tested. The results indicate that there is not a detectable difference in the evolution of the interface temperature for the range of Reynold numbers tested.

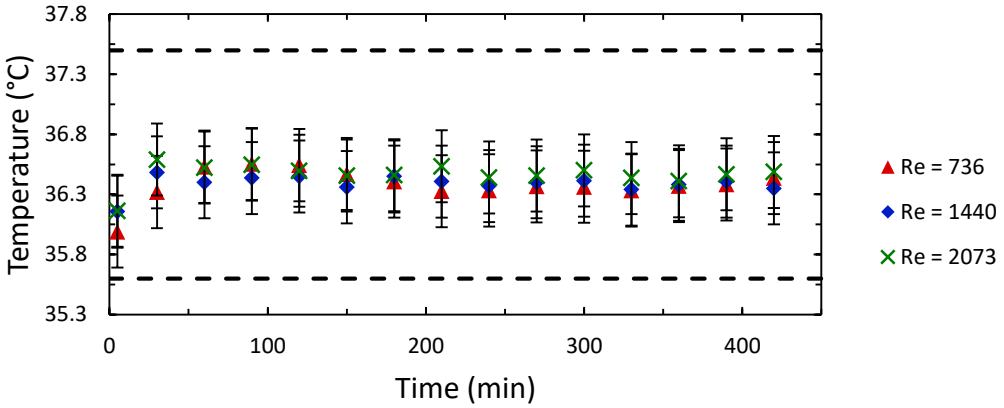

Figure 7: Time evolution of the deposit-liquid interface temperature for different Reynolds numbers for the high cooling rate experiments.

In order to investigate the initial stages of the deposition that presented a significant lower value for the interface temperature, additional experiments were performed. In these experiments, instead of lowering the probe until reaching the deposit-liquid interface, the miniature probe was pre-positioned at distances of 1, 2 and 3 mm from the copper pipe wall. This different method was employed due to the fast growth rate of the deposit that did not allow for the necessary time to precisely position the temperature probe at the interface. After the initiation of the deposition process, simultaneous registration of images for the probe temperature were performed. The deposit-liquid interface temperature could be determined by observing the frame-by-frame images of the 100-µm probe junction being engulfed by the deposit interface. The temperature value corresponding to each image frame was known from the synchronized records. The results of the measurements obtained with this methodology can be seen in Figure 8. It is interesting to observe in the figure that the deposit-liquid interface temperature, for all three Reynolds number investigated, matched the exact value of the WAT. In Figure 8, the measurements for time equal to 5 minutes obtained with the technique based on probe motion are also presented. The initiation of the interface temperature increase toward the constant value reported in Figures 4 to 6 can be observed. It can also be noted that the time to reach the predetermined positions of the probe tip increases with Reynolds number.

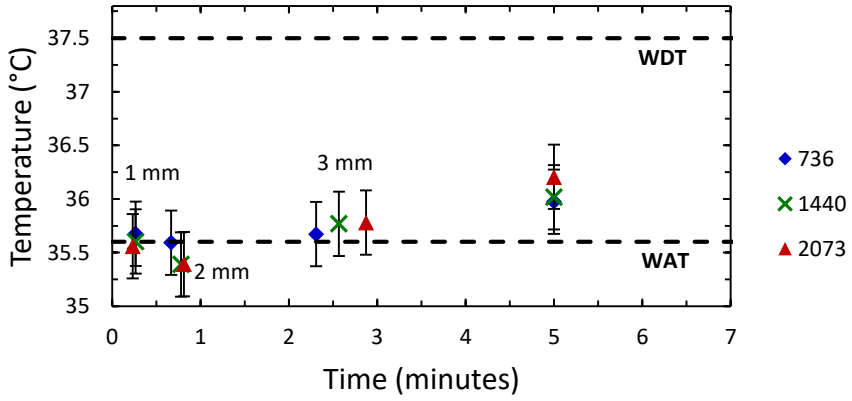

Figure 8. Deposit-liquid interface temperature for pre-determined positions of the thermocouple probe, for Reynolds numbers of 736, 1440 and 2073.

As could be seen in the results presented here, the deposit-liquid interface temperature measurements were never bellow the WAT, and therefore, a concentration gradient could not be formed. This information contradicts that molecular diffusion is the dominant mechanism on wax deposition. The fact that the temperature measurements performed at the first five minutes of deposition are equal to the WAT, indicate that heat transfer, in this case, is the main responsible for the formation and growth of the wax deposits.

For longer deposition times, the deposit interface, however, did not follow the exact value of the WAT, as predicted by the supporters of the heat transfer approach. The interface temperature value presented an increase from the WAT to a value between the WAT and the WDT.

A possible explanation for the observed behavior of the interface temperature is related to necessary subcooling for wax precipitation. This degree of supercooling was found to be directly proportional to the cooling rate, that is, as the

cooling rate increases, the greater the supercooling required (Andrade et al., 2017). For the higher cooling rate that prevail in initial stages of the experiment, the subcooling associated with the WAT promotes wax formation. As the cooling rate is reduced due to the thermal insulation provided by the deposit, a lower degree of subcooling is required and crystal form at a higher temperature.

Another explanation for the interface temperature being different from the WAT and WDT is the possible local variation of the fluid original composition which would lead to a different local value for the WAT and WDT. Indeed, Veiga et al., 2020 have presented numerically predicted concentration profiles of the heavier wax components where the increase in the concentration of these components in the fluid above the interface was evident. Further investigation is necessary to address this issue.

3.2 Visulaization of wax crystal formation

The deposit formation process was recorded by the same high resolution camera used in the measurements of the deposit-liquid interface temperature. While performing the deposit-liquid interface temperature measurements, suspended wax crystals flowing above the deposit were observed. This wax crystals cloud appeared only during the initial stages of the deposit growth. In order to investigate the origin of these crystals and verify that they were not just being detached from upstream regions, the camera that was initially located at a dimensionless axial position x/L=0.8 was moved to an upstream x/L = 0.2.

Two frames extracted from the recorded video at different times of the annular region at the axial position of x/L=0.2 are presented in Figure 9. Figure 9(a) shows the beginning of the experiments without the presence of solid wax deposit. The dark region at the bottom is the copper pipe, and above it is the annular region where the waxy oil flows. It is possible to see in Figure 9(b) that the suspended wax crystals still appeared, indicating that its occurrence is unrelated to the shear stress imposed by the flow over an already formed deposit. The deposition process at the cooling rate of 0.5°C/min was found to always present three different stages: Precipitation of small crystals above the clean copper pipe; Increase in size and number of wax crystals and finally, after the deposit had grown to form a thick layer, the number of crystals decrease until completely vanishing. During this process, however, the deposit growth was not linear with time. After the initial precipitation, some crystals would attach to the copper wall, while others would seem to be formed and grow already attached to it. Either way, these initially attached solids eventually were stripped from the wall due to the shear forces of the flow, indicating a competition between the yield stress of this agglomerate of solids and the shear stress imposed by the flow. Once the copper pipe became colder and the amount of solids increased, a deposit would be formed without detaching, finally being able to resist the flow-induced forces. This results indicates that the rheological beahavior of the desposits should considered in the development of wax deposition models.

(a)

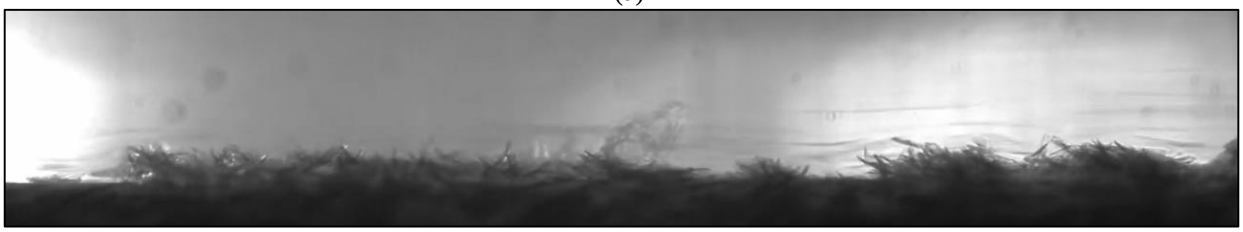

(b)

Figure 9. Instantaneous images of the deposit formations where (a) is the clean annular region, before the beginning of the deposition and (b) is the initial deposition with suspended wax crystals flowing above the deposit.

`

4. CONCLUSIONS

The present work provided valuable information regarding the physical mechanisms involved in the process of wax deposition on cold surfaces. This study followed the research strategy of carrying out experiments with simple geometries and using a model fluid with well-known properties. In addition, the experimental test section was carefully developed to provide well-defined boundary conditions, allowing measurements to be taken while wax deposition experiments were running.

In this work, measurements were performed for the temperature of the deposit-liquid interface. The experiments were performed for three different Reynolds numbers, namely, 736, 1440 and 2073.

Measurements of the temporal evolution of the temperature of the deposit-liquid interface indicate that the interface is initially at the WAT increasing to a constant value between the WAT and the WDT. As the deposit-liquid interface temperature is always above the WAT, this result contradicts the most commonly employed molecular diffusion based wax deposition models. The evolution of the deposit interface at the WAT for the initial times is a strong evidence that the deposition could occur only by heat transfer for the conditions tested. The Reynolds number did not have any influence on the temperature of the deposit interface.

The presence of suspended wax crystals flowing above the deposit was investigated with images recorded with a high frame rate camera. The initial appearance of this "cloud of crystals" was found to be unrelated to crystals detached upstream. These orginal images indicate that a competition between the yield stress of the newly formed deposit and the shear forces imposed by the flow might be relevant to deposit formation

5. ACKNOWLEDGEMENTS

The authors acknowledge the support awarded to this research by the Brazilian Government agencies, CNPq and CAPES, by the Petrobras and TotalEnergies.

6. REFERENCES

Alhosani, A., & Daraboina, N. (2020). Unified Model to Predict Asphaltene Deposition in Production Pipelines. *Energy and Fuels*, *34*(2), 1720–1727. https://doi.org/10.1021/acs.energyfuels.9b04287

Andrade, D. E. V., Marcelino Neto, M. A., & Negrão, C. O. R. (2017). The importance of supersaturation on determining the solid-liquid equilibrium temperature of waxy oils. *Fuel*, *206*, 516–523. https://doi.org/10.1016/j.fuel.2017.06.042

Azevedo, L. F. A., & Teixeira, A. M. (2003). A critical review of the modeling of wax deposition mechanisms. *Petroleum Science and Technology*, *21*(3–4), 393–408. https://doi.org/10.1081/LFT-120018528

Bhat, N. V., & Mehrotra, A. K. (2004). Measurement and prediction of the phase behavior of wax-solvent mixtures: Significance of the wax disappearance temperature. *Industrial and Engineering Chemistry Research*, *43*(13), 3451–3461. https://doi.org/10.1021/ie0400144

Bidmus, H., & Mehrotra, A. K. (2008a). Measurement of the liquid-deposit interface temperature during solids deposition from wax-solvent mixtures under static cooling cconditions. *Energy and Fuels*, *22*(6), 1174–1182. https://doi.org/10.1021/ef800542a

Bidmus, H., & Mehrotra, A. K. (2008b). Measurements of the liquid-deposit interface temperature during solid deposition from wax-solvent mixtures under static cooling conditions. *Energy and Fuels*, *22*(6), 4039–4048. https://doi.org/10.1021/ef800542a

Bidmus, H. O., & Mehrotra, A. K. (2004). Heat-Transfer Analogy for Wax Deposition from Paraffinic Mixtures. *Industrial and Engineering Chemistry Research*, *43*(3), 791–803. https://doi.org/10.1021/ie030573v

Burger, E. D., Perkins, T. K., & Striegler, J. H. (1981). Studies of Wax Deposition in the Trans Alaska Pipeline. *JPT, Journal of Petroleum Technology*, *33*(6), 1075–1086. https://doi.org/10.2118/8788-PA

Ehsani, S., Haj-Shafiei, S., & Mehrotra, A. K. (2019a). Deposition from waxy mixtures in a flow-loop apparatus under turbulent conditions: Investigating the effect of suspended wax crystals in cold flow regime. *Canadian Journal of Chemical Engineering*, *97*(10), 2740–2751. https://doi.org/10.1002/cjce.23570

Ehsani, S., Haj-Shafiei, S., & Mehrotra, A. K. (2019b). Experiments and modeling for investigating the effect of suspended wax crystals on deposition from 'waxy' mixtures under cold flow conditions. *Fuel*, *243*(January), 610–621. https://doi.org/10.1016/j.fuel.2019.01.089

Ehsani, S., & Mehrotra, A. K. (2019). Validating Heat-Transfer-Based Modeling Approach for Wax Deposition from Paraffinic Mixtures: An Analogy with Ice Deposition. *Energy and Fuels*, *33*(3), 1859–1868. https://doi.org/10.1021/acs.energyfuels.8b03777

Ehsani, S., & Mehrotra, A. K. (2020). Investigating the gelling behaviour of 'waxy'' paraffinic mixtures during flow shutdown.' *Canadian Journal of Chemical Engineering*. https://doi.org/10.1002/cjce.23811

Gao, X., Huang, Q., Zhang, X., Zhang, Y., Zhu, X., & Shan, J. (2021). Experimental study on the wax removal physics of foam pig in crude oil pipeline pigging. *Journal of Petroleum Science and Engineering*, *205*(April), 108881. https://doi.org/10.1016/j.petrol.2021.108881

Haj-Shafiei, S., & Mehrotra, A. K. (2019). Achieving cold flow conditions for 'waxy' mixtures with minimum solid

deposition. *Fuel*, *235*(July 2018), 1092–1099. https://doi.org/10.1016/j.fuel.2018.08.102

Hamouda, A. A., & Ravnøy, J. M. (1992). Prediction of wax deposition in pipelines and field experience on the influence of wax on drag-reducer performance. *Proceedings of the Annual Offshore Technology Conference*, *1992-May*, 669–679. https://doi.org/10.4043/7060-ms

Hoffmann, R., & Amundsen, L. (2010). Single-phase wax deposition experiments. *Energy and Fuels*, *24*(2), 1069–1080. https://doi.org/10.1021/ef900920x

Hoteit, H., Banki, R., & Firoozabadi, A. (2008). Wax deposition and aging in flowlines from irreversible thermodynamics. *Energy and Fuels*, *22*(4), 2693–2706. https://doi.org/10.1021/ef800129t

Huang, Z., Su Lee, H., Senra, M., & Fogler, S. (2011). A Fundamental Model of Wax Deposition inSubsea Oil Pipelines. *AIChE Journal*, *59*(4), 215–228. https://doi.org/10.1002/aic

Mahir, L. H. A., Vilas Bôas Fávero, C., Ketjuntiwa, T., Fogler, H. S., & Larson, R. G. (2019). Mechanism of Wax Deposition on Cold Surfaces: Gelation and Deposit Aging. *Energy and Fuels*, *33*(5), 3776–3786. https://doi.org/10.1021/acs.energyfuels.8b03139

Mehrotra, A. K., & Bhat, N. V. (2007). Modeling the effect of shear stress on deposition from "Waxy" mixtures under laminar flow with heat transfer. *Energy and Fuels*, *21*(3), 1277–1286. https://doi.org/10.1021/ef060445u

Mehrotra, A. K., Ehsani, S., Haj-Shafiei, S., & Kasumu, A. S. (2020). A review of heat-transfer mechanism for solid deposition from "waxy" or paraffinic mixtures. *Canadian Journal of Chemical Engineering*. https://doi.org/10.1002/cjce.23829

Merino-Garcia, D., Margarone, M., & Correra, S. (2007). Kinetics of waxy gel formation from batch experiments. *Energy and Fuels*, *21*(3), 1287–1295. https://doi.org/10.1021/ef060385s

Palermo, T., & Tournis, E. (2015). Viscosity prediction of waxy oils: Suspension of Fractal Aggregates (SoFA) model. *Industrial and Engineering Chemistry Research*, *54*(16), 4526–4534. https://doi.org/10.1021/ie504166n

Parthasarathi, P., & Mehrotra, A. K. (2005). Solids deposition from multicomponent wax-solvent mixtures in a benchscale flow-loop apparatus with heat transfer. *Energy and Fuels*, *19*(4), 1387–1398. https://doi.org/10.1021/ef0497107

Singh, P., Venkatesan, R., Fogler, H. S., & Nagarajan, N. (2000). Formation and aging of incipient thin film wax-oil gels. *AIChE Journal*, *46*(5), 1059–1074. https://doi.org/10.1002/aic.690460517

Singh, P., Youyen, A., & Fogler, H. S. (2001). Existence of a critical carbon number in the aging of a wax-oil gel. *AIChE Journal*, *47*(9), 2111–2124. https://doi.org/10.1002/aic.690470921

Soedarmo, A. A., Daraboina, N., & Sarica, C. (2017). Validation of wax deposition models with recent laboratory scale flow loop experimental data. *Journal of Petroleum Science and Engineering*, *149*, 351–366. https://doi.org/10.1016/j.petrol.2016.10.017

Tiwary, R., & Mehrotra, A. K. (2009). Deposition from wax-solvent mixtures under turbulent flow: Effects of shear rate and time on deposit properties. *Energy and Fuels*, *23*(3), 1299–1310. https://doi.org/10.1021/ef800591p

Van Der Geest, C., Guersoni, V. C. B., Merino-Garcia, D., & Bannwart, A. C. (2018). Wax Deposition Experiment with Highly Paraffinic Crude Oil in Laminar Single-Phase Flow Unpredictable by Molecular Diffusion Mechanism. *Energy and Fuels*, *32*(3), 3406–3419. https://doi.org/10.1021/acs.energyfuels.8b00269

van der Geest, C., Melchuna, A., Bizarre, L., Bannwart, A. C., & Guersoni, V. C. B. (2021). Critical review on wax deposition in single-phase flow. *Fuel*, *293*(March), 120358. https://doi.org/10.1016/j.fuel.2021.120358

Veiga, H. M. B., Boher e Souza, L., Fleming, F. P., Ibanez, I., Linhares, R. C., Nieckele, A. O., & Azevedo, L. F. A. (2020). Experimental and Numerical Study of Wax Deposition in a Laboratory-Scale Pipe Section under Well-Controlled Conditions. *Energy & Fuels*, *34*(10), 12182–12203. https://doi.org/10.1021/acs.energyfuels.0c01316

Yang, J., Lu, Y., Daraboina, N., & Sarica, C. (2020). Wax deposition mechanisms: Is the current description sufficient? *Fuel*, *275*(April). https://doi.org/10.1016/j.fuel.2020.117937

Zheng, S., Saidoun, M., Palermo, T., Mateen, K., & Fogler, H. S. (2017). Wax Deposition Modeling with Considerations of Non-Newtonian Characteristics: Application on Field-Scale Pipeline. *Energy and Fuels*, *31*(5), 5011–5023. https://doi.org/10.1021/acs.energyfuels.7b00504

7. RESPONSIBILITY NOTICE

The authors are the only responsible for the printed material included in this paper.